INNOVATIVE METHODOLOGY FOR DETECTION OF FRACTURE-CONTROLLED SWEET SPOTS IN THE NORTHERN APPALACHIAN BASIN

June 1, 2000-March 31, 2007

TOPICAL REPORT #9

First Draft: June 30, 2007

Dr. Robert Jacobi, Principal Author

DE-AC26-00NT40698

CONTRACTOR:
Research Foundation of State University of New York
P. O. Box 9
Albany, New York 12201
on behalf of:
University at Buffalo
The State University of New York
Suite 211, The UB Commons
520 Lee Entrance
Amherst, New York 14228

Dr. Robert Jacobi, Project Director
Dr. John Fountain, Co-Principal Investigator

Mr. Stuart Loewenstein, Subcontractor
Nornew, Inc
1412 Sweet Home Road, Suite 12
Amherst, NY 14228

Dr. Edward deRidder, Subcontractor
Pearson, deRidder and Johnson, Inc.
12640 West Cedar Drive, Suite 100
Lakewood, CO 80228

Dr. Bruce Hart, Subcontractor
Earth and Planetary Sciences
McGill University
3450 University Street
Montreal, Quebec
Canada H3A 2A7

DISCLAIMER

ABSTRACT

This Topical Report (#9 of 9) consists of the figures 3.8-1 to (and including) 3.9-5 (and appropriate figure captions) that accompany the Final Technical Progress Report entitled: "Innovative Methodology for Detection of Fracture-Controlled Sweet Spots in the Northern Appalachian Basin" for DOE/NETL Award DE-AC26-00NT40698.

TABLE OF CONTENTS

LIST OF GRAPHICAL MATERIALS

LIST OF TABLES

FIGURE CAPTIONS FOR TOPICAL REPORT #8

FIGURE 3.8-1. **Reassembled, Oriented, Horizontal Core from the Black River in Central New York State.**
Rotation of individual core segments were rotated to match FMI log.

FIGURE 3.8-2. **Porosity and Permeability Determinations of Full Core Segments**.
The upper panel shows porosity measurement, and the lowest panel shows permeability values. The middle panel indicates the type of feature tested, stylolite, porous bedding, vugs, and normal (dense) bedding.

FIGURE 3.8-3. **Orientations of Veins Measured on the Full Core (Before Slabbing).**
Stereonets in upper panels display orientations of veins. Histogram of vein orientations in the lower panel defines the boundaries of the orientation sets (e.g., NE-trending veins strike between 45^0 and 65^0); boundaries of sets based on natural distribution breaks and vein characteristics (e.g., intersection relationships).

FIGURE 3.8-4. **Orientations of Stylolites Measured on the Full Core (Before Slabbing).**
Stereonets in upper panels display orientations of stylolites. Histogram of stylolites orientations in the lower panel defines the boundaries of the orientation.

FIGURE 3.8-5. **Cross-Cutting Plot for all Stylolites and Veins Collected from Full-Diameter Core and Slab.**
The X-axis is the strike of a feature observed to cut another feature and therefore is younger. The Y-axis is the strike of a feature seen to be cut by another feature and therefore older. The symbols show which type of feature is cut and being cut. Clusters defined in the upper left (red and green outlines) wherein the cutting veins trend between 25^0 and 50^0 do not have well defined inverse relationships (wherein the cut features trend between 25^0 and 50^0).

FIGURE 3.8-6. **Sketches of Kinematic Indicators from the Full Core.**
Lines within the rhombochasm indicate crystal growth direction. All features shown here are releasing bends (transtensional rhombochasms). The photo is of feature #112 and shows the geometry of these types of features. The stick diagram in the lower right shows a composite of the sense of offsets observed on all veins of varying orientation. The red feature is youngest, followed by green, and blue is the oldest. The black features in this composite are of undetermined relative age.

FIGURE 3.8-7. **Sketches of Additional Kinematic Indicators from the Slabbed Core.**
Lines within the rhombochasm indicate crystal growth direction. Features A and 9 are restraining bends (zones of transpression) as shown in the

upper photo of feature A. The offsets of features B, C, and D were determined by consistent twists as shown in the middle photo of feature B. Feature 112 is a transtensional rhombochasm as illustrated in the lower photo. The offsets of features 14 and E were determined by crystal growth orientations oblique to the vein opening direction. The sketch in the lower right shows a composite of the sense of offsets observed on all veins of varying orientation. Double arrows indicate two features showing the same slip. The red feature is youngest, followed by green, and blue is the oldest. The black features in this composite are of undetermined relative age.

FIGURE 3.9-1. **Structure Contour Map on the Devonian Rhinestreet and Landsat Lineaments.**
Structure from Bradley et al. (1941) and Lineaments from EarthSat (1997).

FIGURE 3.9-2. **Aeromagnetics (RTP), EarthSat (1997) Lineaments and Selected T/BR Gas Fields.**
A) Map shows individual lineaments (in white) and T/BR discovery fields in red (original extent) and more recent extent (purple). B) Map shows overlay of lineament bundles (yellow zones) that probably mark fault systems.

FIGURE 3.9-3. **Landsat Lineaments and Selected Trenton/Black River Fields. Lineaments from EarthSat (1997).**

FIGURE 3.9-4. **Orientation of Structural Features During "Middle" Taconic Times (Before the Laurentian Plate had Jammed the Subduction Zone).**
A) Potential extensional features (normal faults and Mode I fractures) are highlighted that could have formed, or been reactivated, under the stress conditions of continental plate flexure over the peripheral bulge and into the trench. Dashed features are oriented less favorably, but would also have been active if they were pre-existing.
B) Potential strike-slip features (strike slip faults and Mode II fractures) are highlighted that could have formed, or been reactivated, under the stress conditions of continental plate flexure over the peripheral bulge and into the trench. Dashed features are oriented less favorably, but would also have been active if they were pre-existing. Right lateral, NW-striking faults are gray, compared to the bold black of the left lateral faults. The strike slip faults probably experienced oblique slip with a down-to-the-east component of slip. In both cases "A" and "B", the inexact orientation of the trench and the relative convergence between the plates makes these diagrams primarily schematic. CLF = Clarendon-Linden Fault System, D = Dolgeville Fault, E = Ephrata Fault, EFBZ = Elzevir-Frontenac Boundary Zone, ESA = East Stone Arabia Fault, GL = Galway Lake Fault, HE = Herkimer Fault, HO = Hoffmans Fault, LF = Little Falls

Fault, MC = Mother Creek Fault, N = Noses Fault. P = Prospect Fault, S = Sprakers Fault, W = West Stone Arabia Fault After Jacobi et al. 2003. (Block diagram after Bradley and Kidd, 1991)

FIGURE 3.9-5. **Orientation of Structural Features During "Late" Taconic Times (During the Laurentian Plate Jamming the Subduction Zone).**
A) Potential extensional features (Mode I fractures) are highlighted that could have formed, or been reactivated, under the stress conditions during final jamming. Dashed features are oriented less favorably, but would also have been active if they were pre-existing.
B) Potential strike-slip features (strike slip faults and Mode II fractures) are highlighted that could have formed, or been reactivated, under the stress conditions of continental plate flexure over the peripheral bulge and into the trench. Dashed features are oriented less favorably, but would also have been active if they were pre-existing. Right lateral, NE-striking faults are gray, compared to the bold black of the left lateral faults. The strike slip faults probably experienced oblique slip with a down-to-the-east component of slip. In both cases "A" and "B", the inexact orientation of the trench and the relative convergence between the plates makes these diagrams primarily schematic. Abbreviations same as in Figure 3.9-4. After Jacobi et al. (2003). (Block diagram after Bradley and Kidd, 1991)

TABLE CAPTIONS

TABLE 2.8-1. **Core Rotations.**

TABLE 2.8-2. **Observed Breaks in Reassembled Core**.

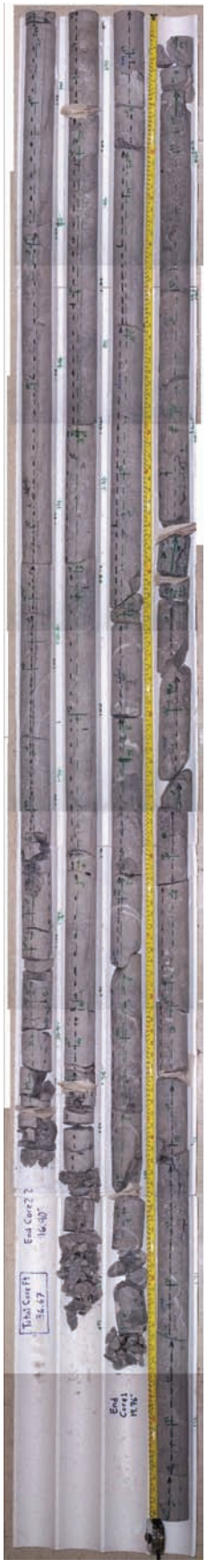

FIGURE 3.8-1

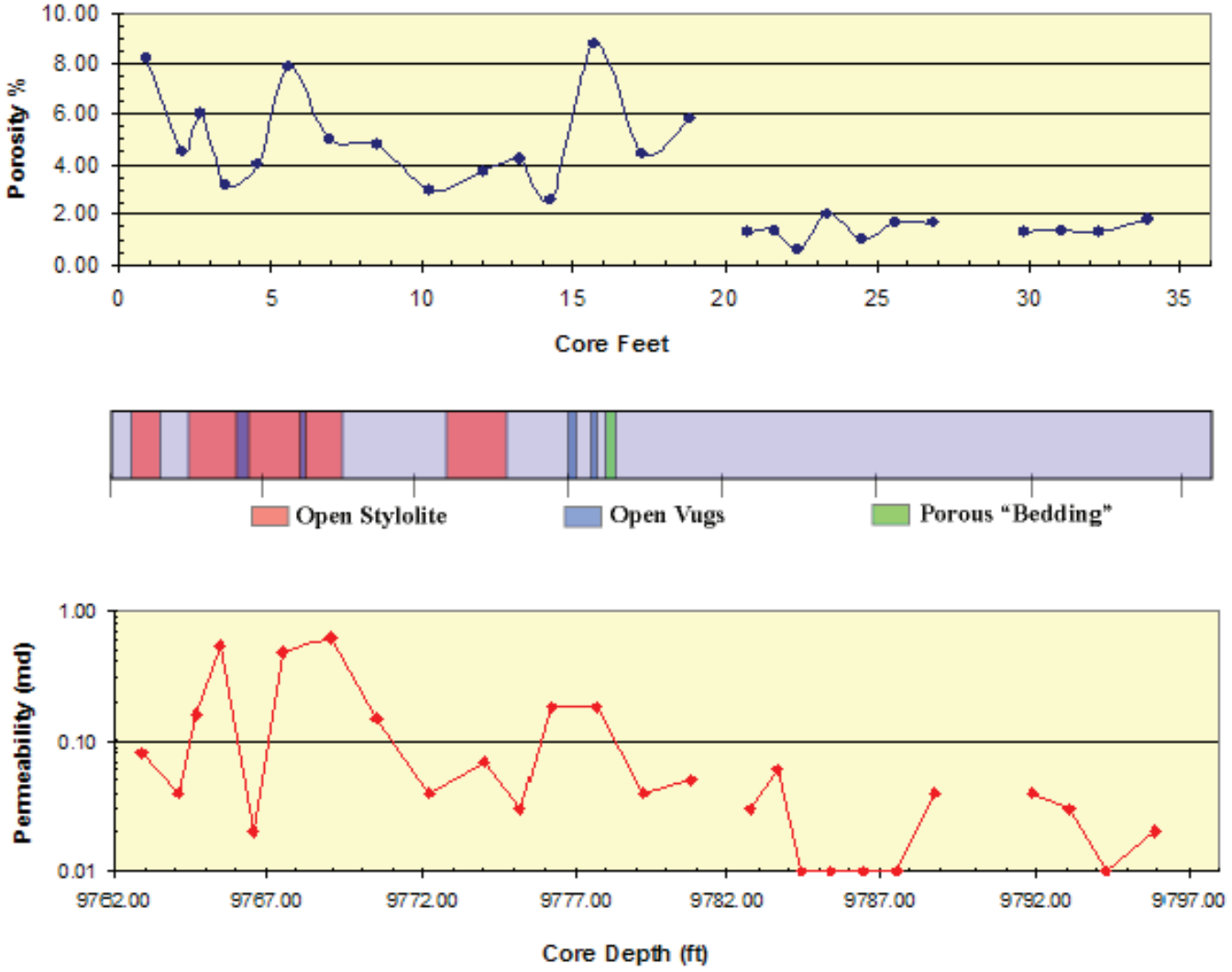
Porosity %
10.00
8.00
6.00
4.00
2.00
0.00
0
5
10
15
20
25
30
35
Core Feet
Open Stylolite
Open Vugs
Porous "Bedding"
Permeability (md)
1.00
0.10
0.01
9762.00
9767.00
9772.00
9777.00
9782.00
9787.00
9792.00
9797.00
Core Depth (ft)

FIGURE 3.8-2

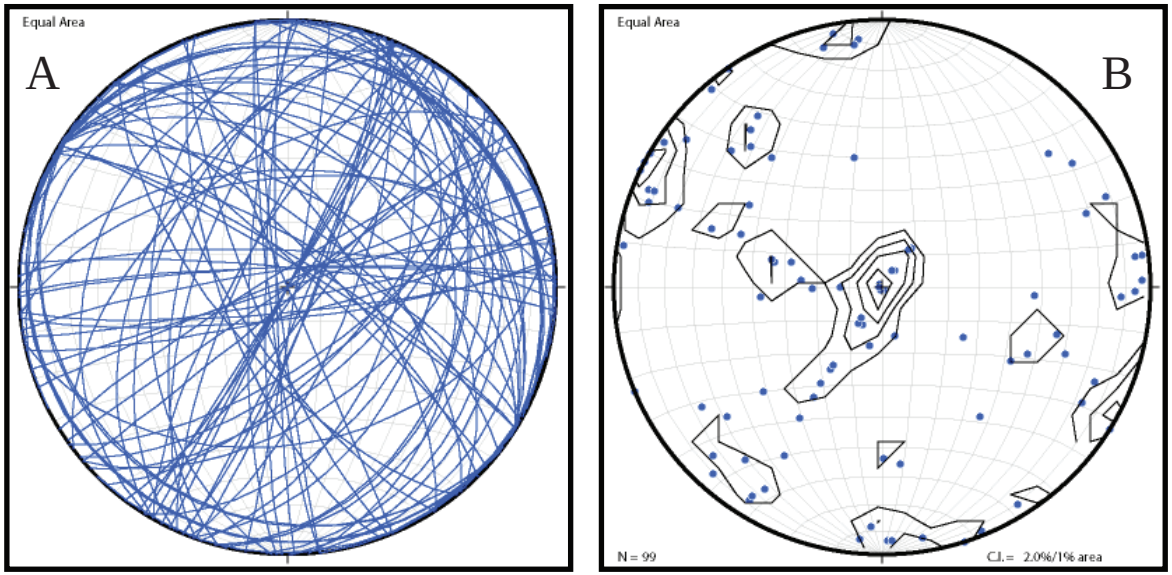
Equal Area
A
Equal Area
B
N = 99
C.I. = 2.0%/1% area

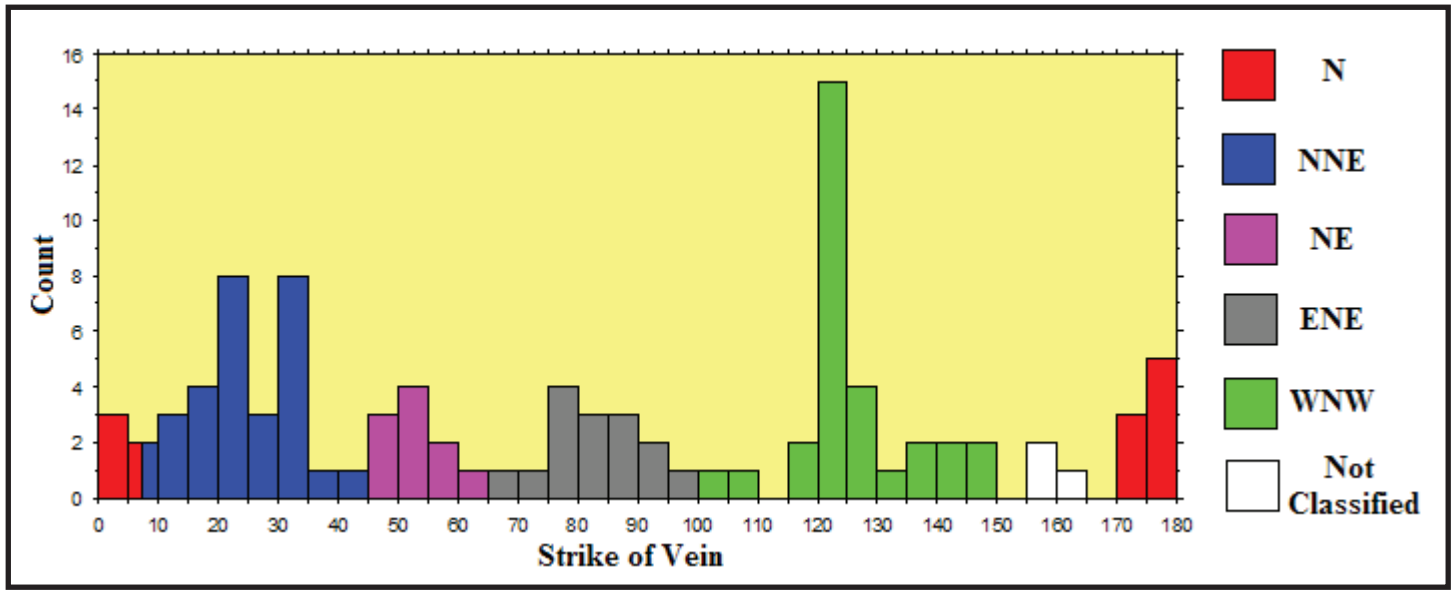
Count
Strike of Vein
0
2
4
6
8
10
12
14
16
0
10
20
30
40
50
60
70
80
90
100
110
120
130
140
150
160
170
180
N
NNE
NE
ENE
WNW
Not Classified

C

FIGURE 3.8-3

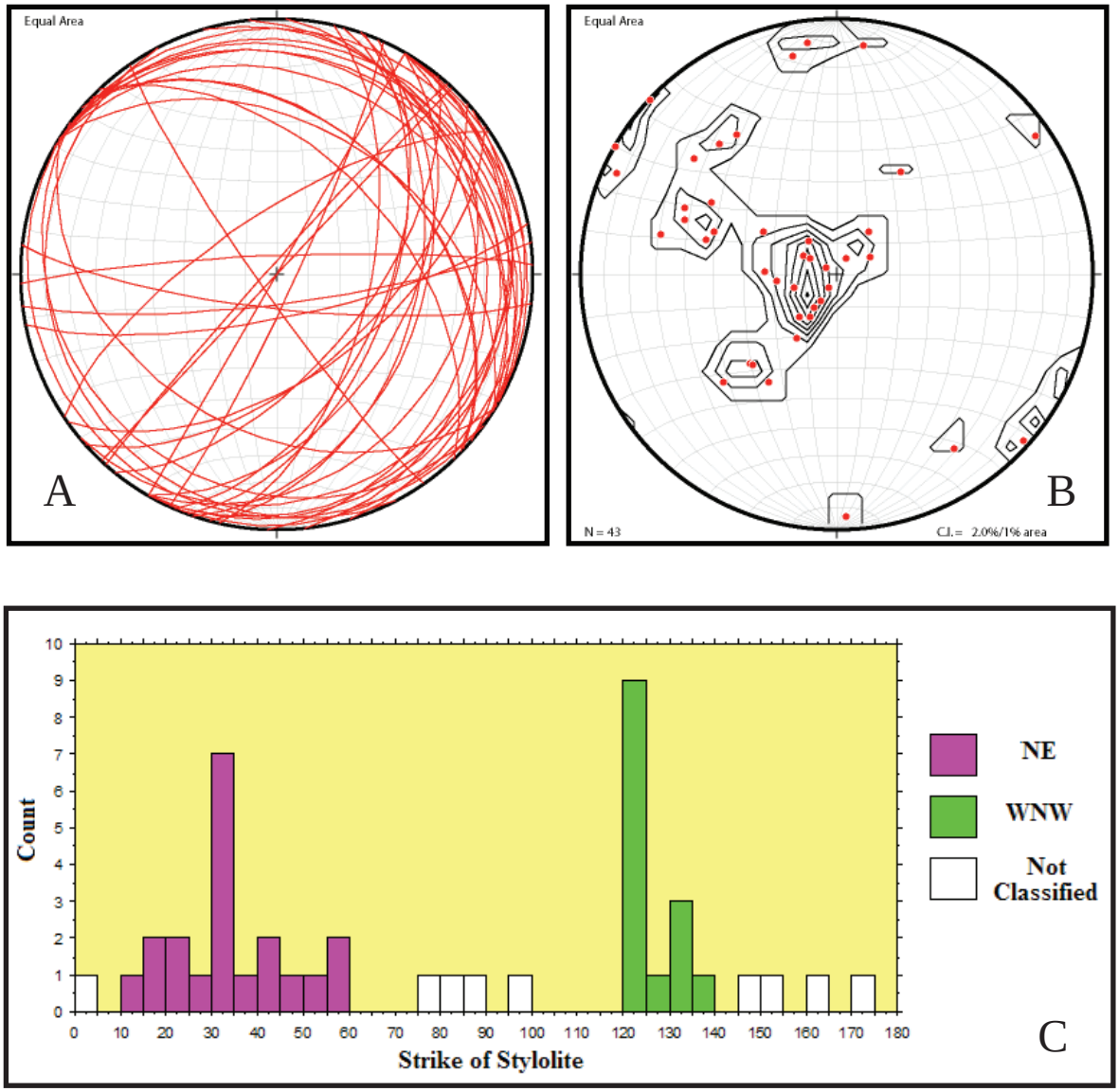
Equal Area
A
Equal Area
B
N = 43
C.I. = 2.0%/1% area
Count
Strike of Stylolite
NE
WNW
Not Classified
C

FIGURE 3.8-4

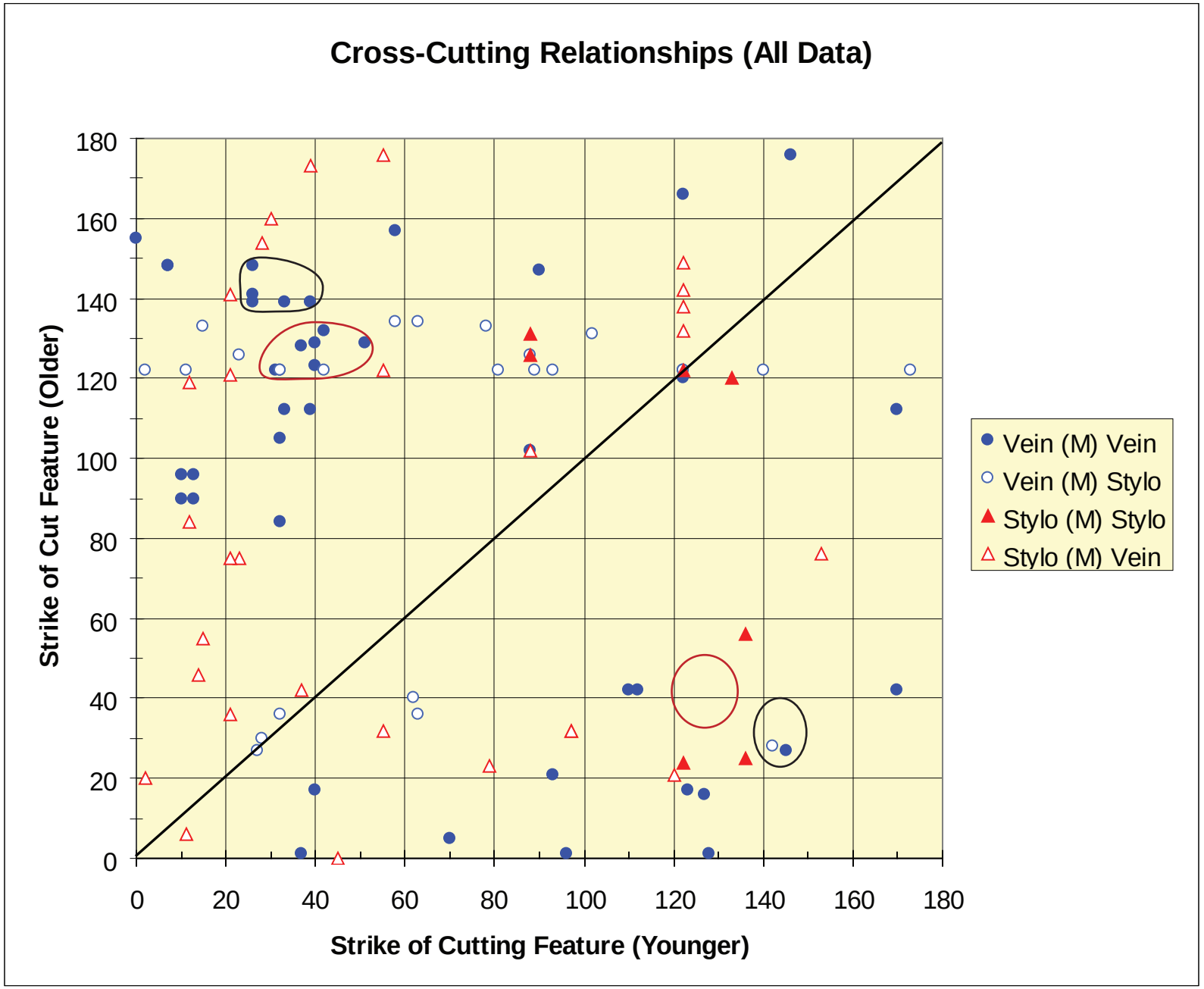
Cross-Cutting Relationships (All Data)
Strike of Cut Feature (Older)
Strike of Cutting Feature (Younger)
0
20
40
60
80
100
120
140
160
180
Vein (M) Vein
Vein (M) Stylo
Stylo (M) Stylo
Stylo (M) Vein

FIGURE 3.8-5

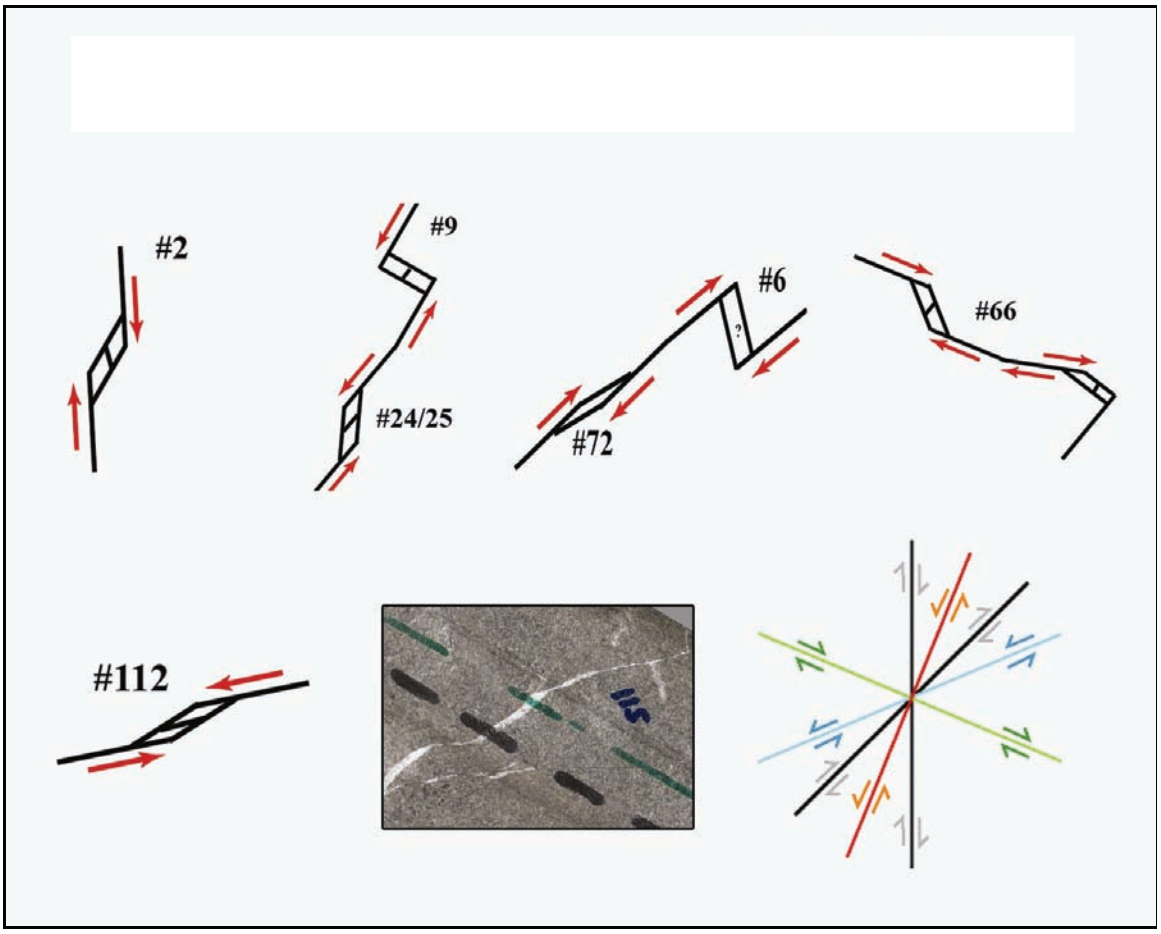

FIGURE 3.8-6

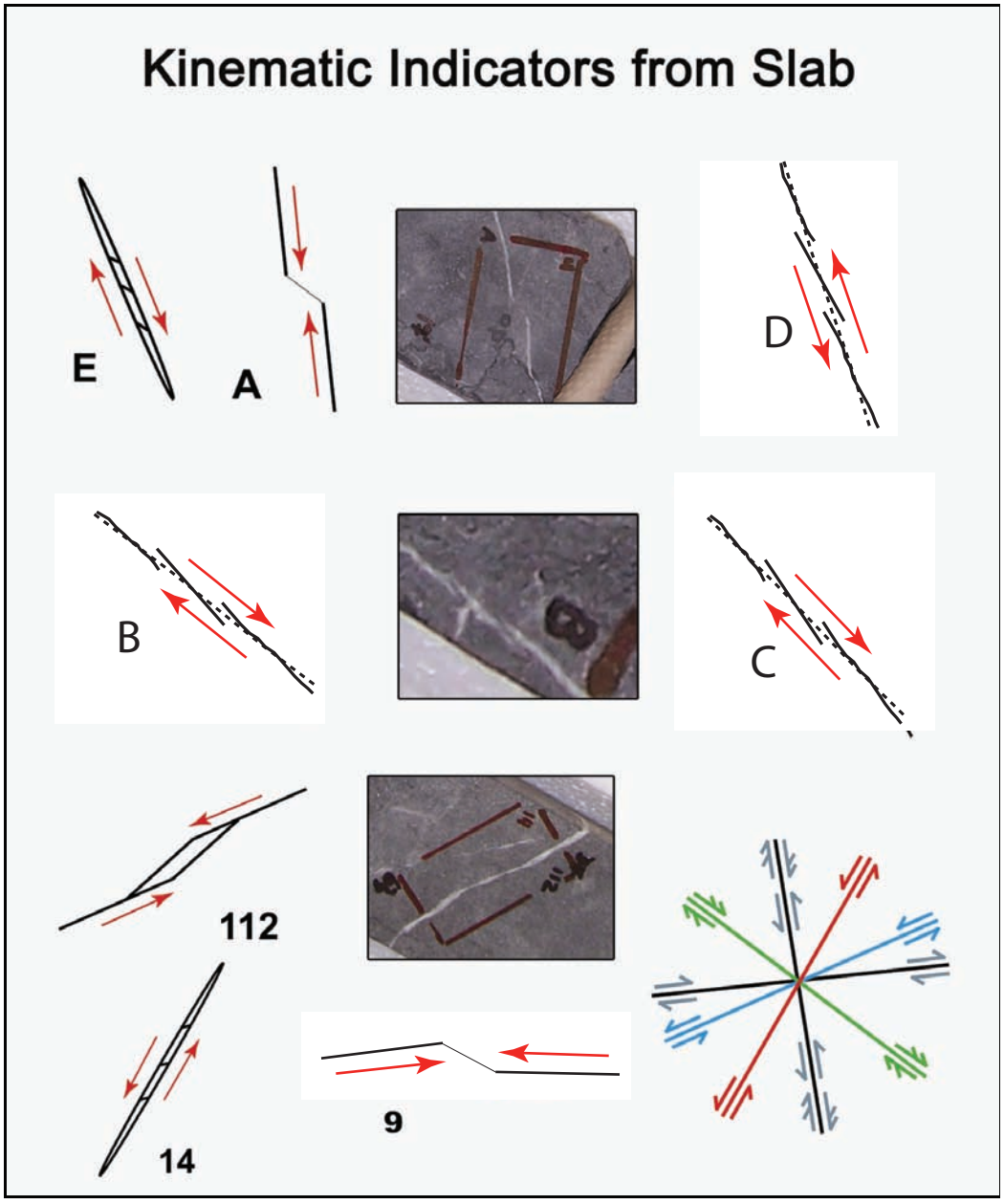

FIGURE 3.8-7

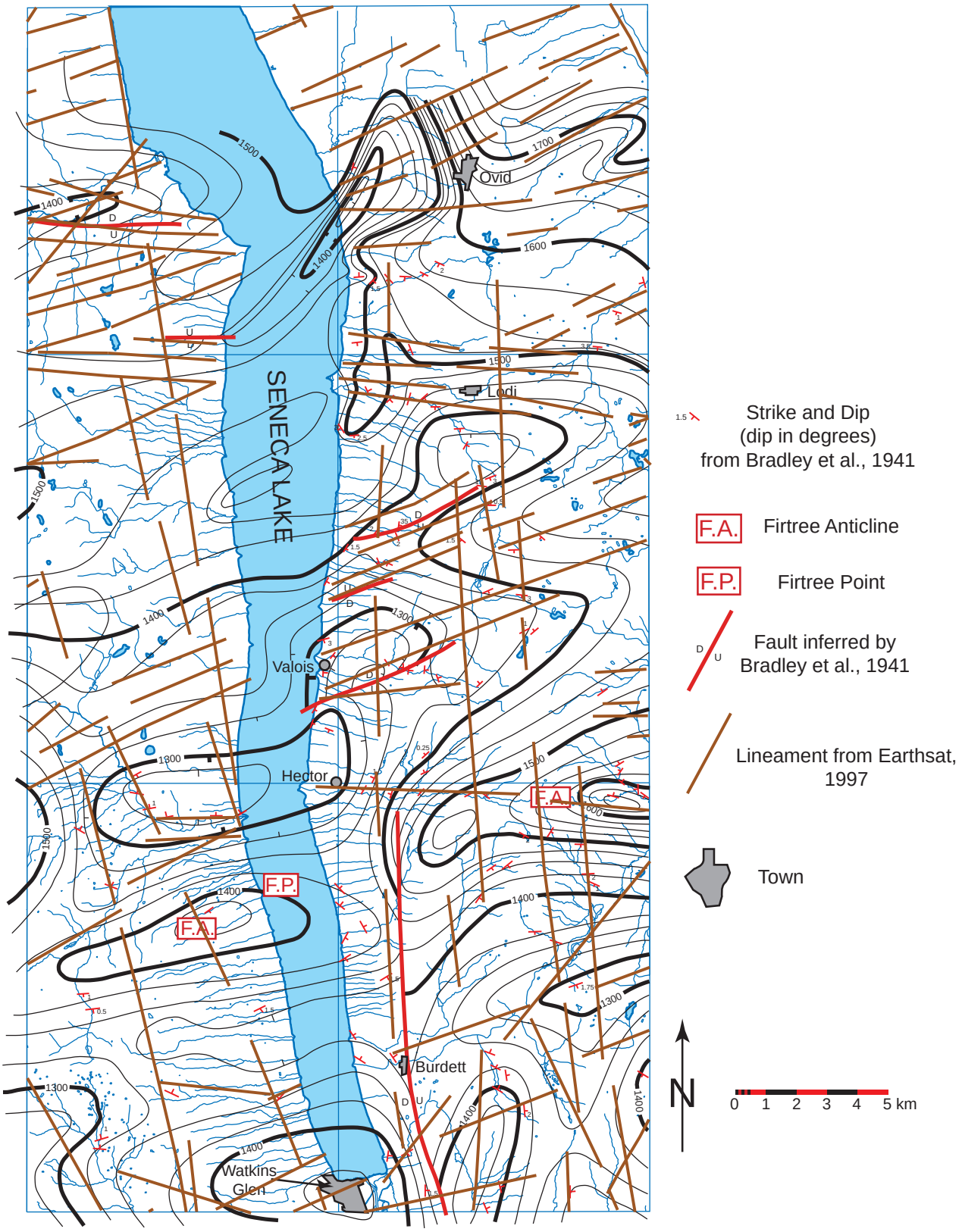
SENECA LAKE
Ovid
Lodi
Valois
Hector
Burdett
Watkins Glen
F.A.
F.P.
F.A.
F.A.
1500
1400
1600
1700
1300
1500
1400
1300
1500
1400
1300
1400
1400
1300
1400
Strike and Dip
(dip in degrees)
from Bradley et al., 1941
F.A. Firtree Anticline
F.P. Firtree Point
D U Fault inferred by
Bradley et al., 1941
Lineament from Earthsat,
1997
Town
N
0 1 2 3 4 5 km

FIGURE 3.9-1

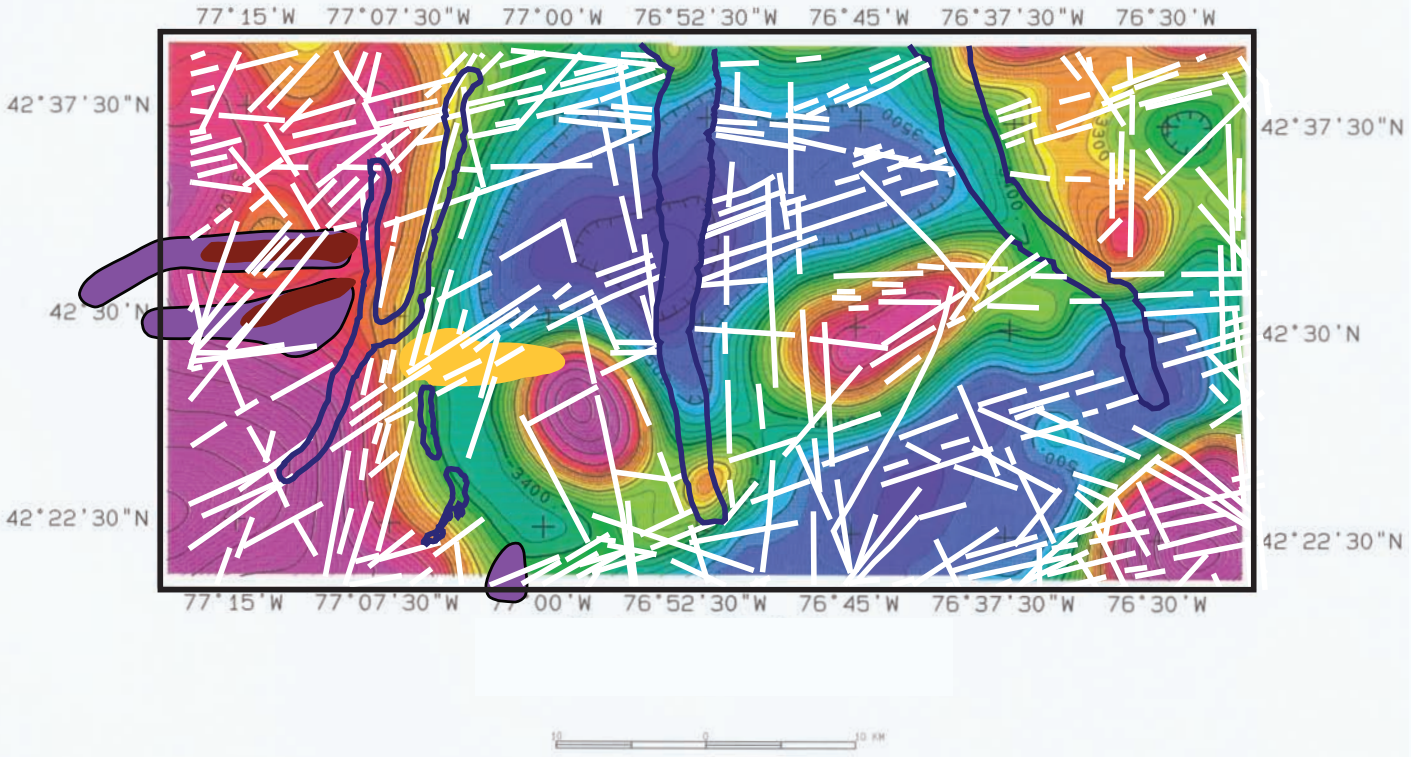

FIGURE 3.9-2a

FIGURE 3.9-2b

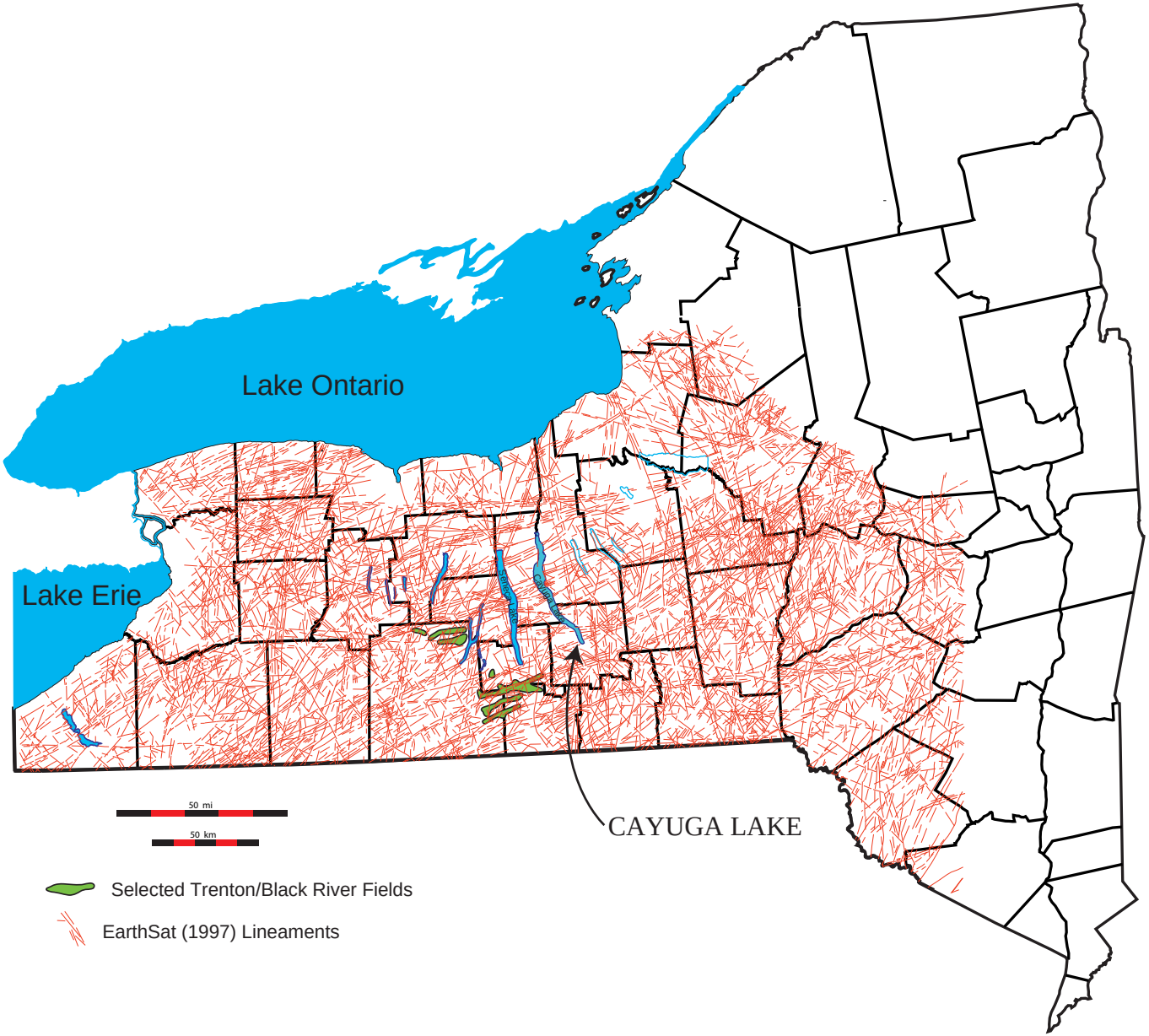
Lake Ontario
Lake Erie
CAYUGA LAKE
50 mi
50 km
Selected Trenton/Black River Fields
EarthSat (1997) Lineaments

FIGURE 3.9-3

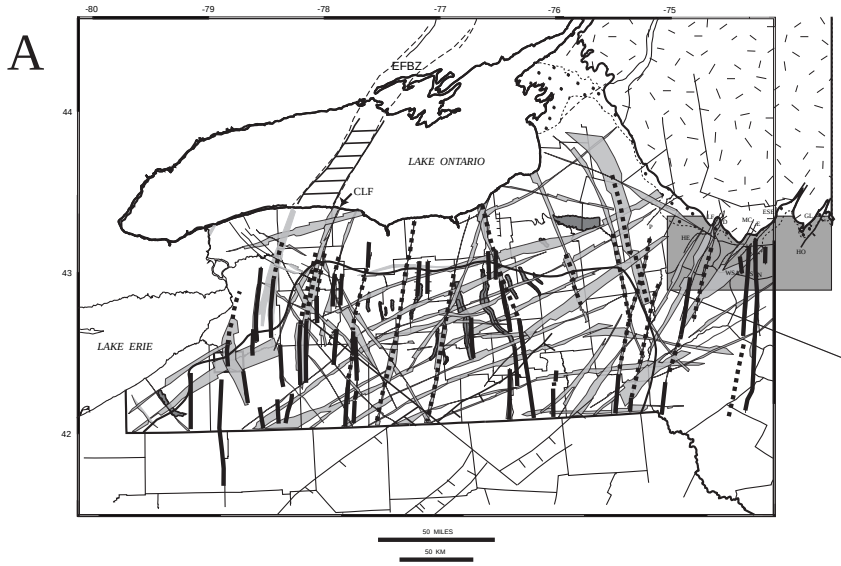

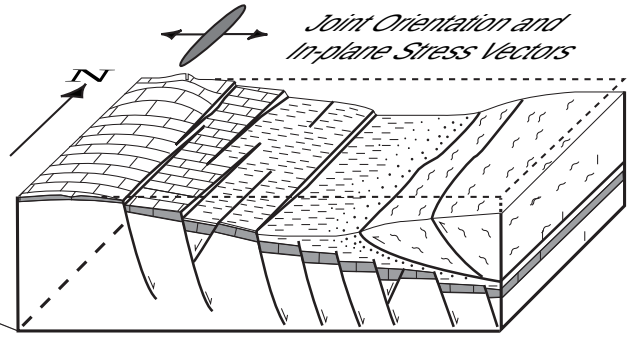

MIDDLE TACONIC
OPEN MODE I JOINTS AND NORMAL FAULTS

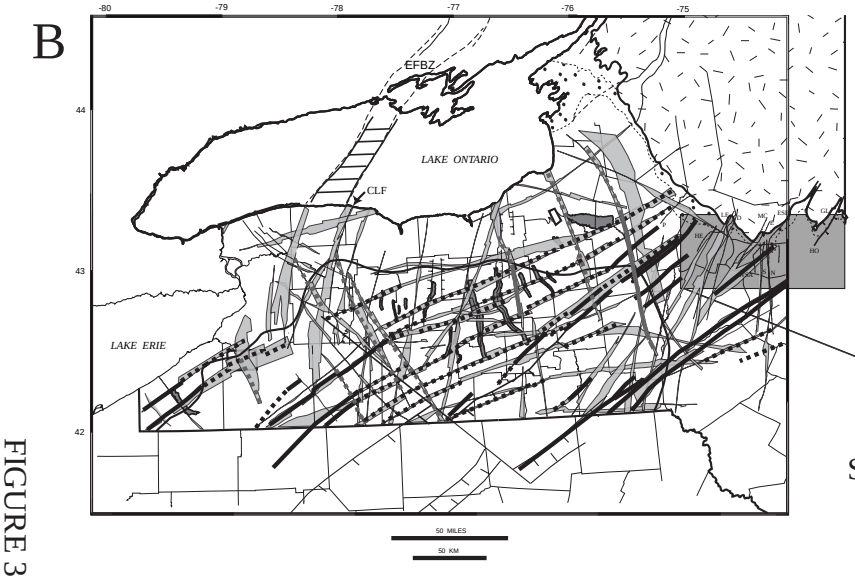

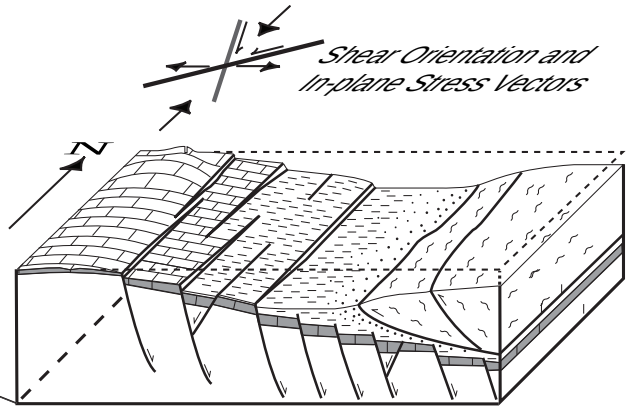

MIDDLE TACONIC
SHEAR (MODE II) JOINTS AND STRIKE SLIP FAULTS

FIGURE 3.9-4

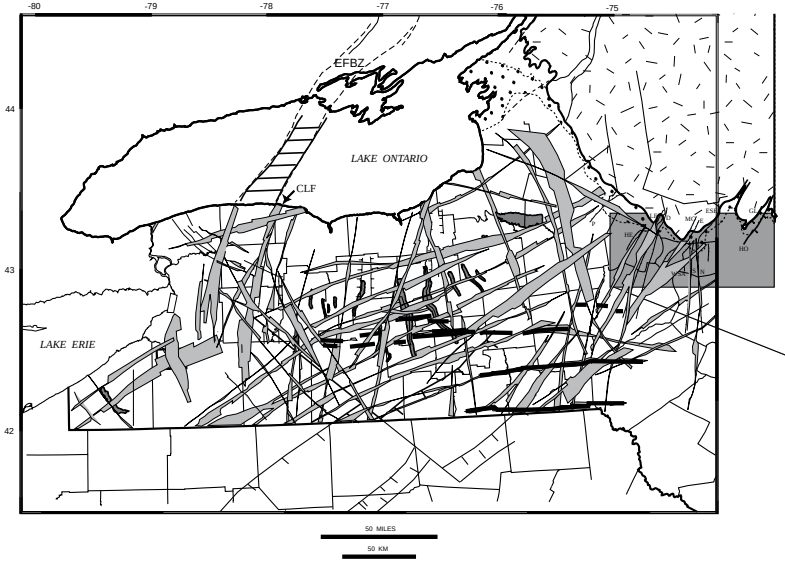

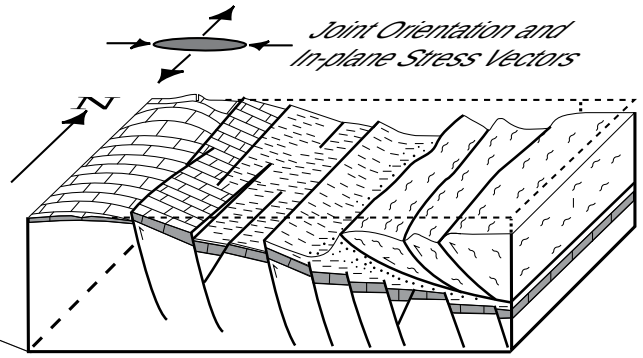

LATE TACONIC
OPEN MODE I JOINTS AND NORMAL FAULTS

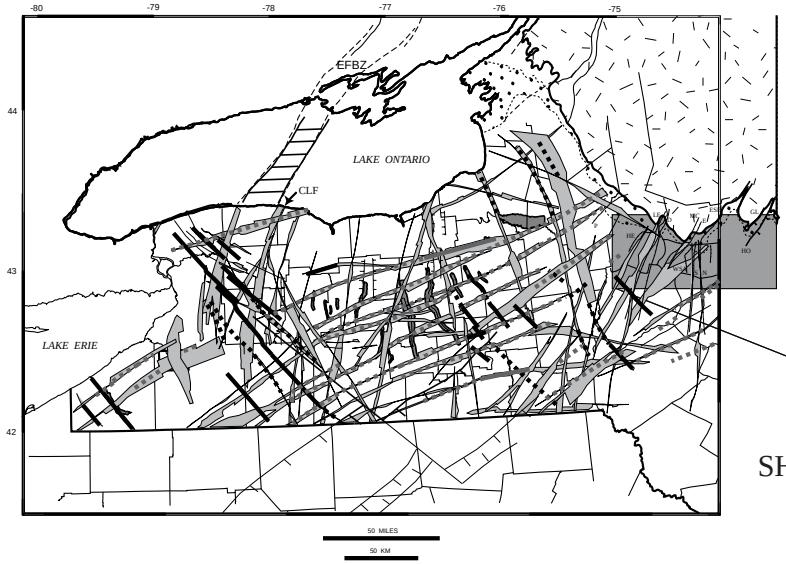

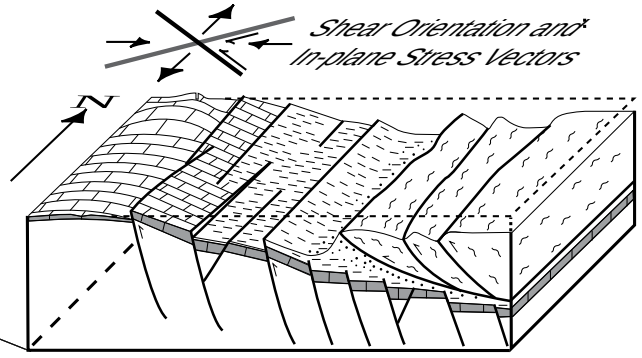

LATE TACONIC
SHEAR (MODE II) JOINTS AND STRIKE SLIP FAULTS

FIGURE 3.9-5

Table 1
Core Rotations From
MagToolFace

DEPTH (in feet)	MagToolFace degrees	
9763	127.89	core 1
9764	208.64	
9767	204.57	
9768	214.5	
9769	222.51	
9770	84.55	
9781	169.17	
9782	335.02	
9783	147.88	

9791	165.93	core 2
9792	328.26	
9793	180.66	
9796	197.86	
9797	207.9	
9801	238.78	
9802	52.49	

TABLE 2.8-1

Table 2
Observed Breaks in Reassembled Core

Continuous Core Feet	Cumulative Core Feet	Depth assuming 9762 start	Comments
3.7	3.7	9765.7	
minor break			
0.29	3.99	9765.99	
minor break			
3.5	7.49	9769.49	
major break			
11.58	19.07	9781.07	
major break			
1.17	20.24	9782.24	rubble
major break			
0.75	20.99	9782.99	
minor break			
6.88	27.87	9789.87	
major break			
1.67	29.54	9791.54	rubble
major break			
6.75	36.29	9798.29	
small chance of spin			
1.04	37.33	9799.33	
major break			
0.42	37.75	9799.75	rubble